Chen et al. *Zool. Res.* 2025, 46(2): 459−468
https://doi.org/10.24272/j.issn.2095-8137.2024.332
https://cstr.cn/32248.14.zr.2024.332

ZR | Zoological Research

Article Open Access

Alterations in the salivary gland microbiota of *Haemaphysalis longicornis* during tick-to-host transmission of severe fever with thrombocytopenia syndrome virus

Jingjing Chen[1,#], Chuanfei Yuan[1,#,*], Qiong Xu[1,#], Yu Sun[1], Rui Zheng[1], Chenghong Zeng[1], Yan Wu[3], Zhen Zou[2,*], Qianfeng Xia[1,*]

[1] *NHC Key Laboratory of Tropical Disease Control*, *School of Tropical Medicine*, *Hainan Medical University*, *Haikou*, *Hainan* 571199, *China*
[2] *State Key Laboratory of Integrated Management of Pest Insects and Rodents*, *Institute of Zoology*, *Chinese Academy of Sciences*, *Beijing* 100101, *China*
[3] *Department of Pathogen Microbiology*, *School of Basic Medical Sciences*, *Capital Medical University*, *Beijing* 100069, *China*

ABSTRACT

Haemaphysalis longicornis serves as the primary tick vector for severe fever with thrombocytopenia syndrome virus (SFTSV), the etiological agent responsible for severe fever with thrombocytopenia syndrome (SFTS). Understanding alterations in tick salivary gland microbiota during SFTSV transmission to vertebrate hosts is essential for developing novel control strategies. However, microbial shifts in tick salivary glands during pathogen transmission to hosts have not been reported for any tick-borne pathogens. In this study, SFTSV transmission from *H. longicornis* to vertebrate hosts was confirmed using a tick-rabbit transmission model. Salivary gland microbiota profiling via 16S rRNA gene sequencing identified significant changes in bacterial composition associated with viral transmission. The relative abundance of three genera (*Serratia*, *Bifidobacterium*, and *Akkermansia*) increased, whereas five genera *(Flavobacterium*, *Staphylococcus*, *Enhydrobacter*, *Massilia*, and *Stenotrophomonas*) decreased. Correlation network analysis revealed a negative association between *Akkermansia* and *Flavobacterium*. These findings demonstrated that SFTSV transmission alters the salivary gland microbiota of *H. longicornis*, providing insights for future functional studies and the development of targeted strategies for SFTS control.

Keywords: SFTSV; Microbiota; Tick; Salivary glands; *Haemaphysalis longicornis*

INTRODUCTION

All metazoans, including ticks, harbor diverse microbiota that contribute to host survival and physiological processes. In ticks, these microbial communities influence development, reproduction, and behavior (Machado-Ferreira et al., 2011; Tsementzi et al., 2018; Zhang et al., 2024; Zhong et al., 2021). Recent studies have suggested that the tick microbiota modulates pathogen acquisition during blood-feeding (Abraham et al., 2017; Narasimhan et al., 2014). Moreover, targeting the tick microbiota through vaccination has been shown to reduce the incidence of pathogen infection in ticks (Wu-Chuang et al., 2023). Understanding microbial dynamics in the context of pathogen transmission could inform novel strategies for controlling tick-borne diseases.

Ticks transmit a wide range of pathogens to vertebrate hosts via blood-feeding (Jia et al., 2020). In nature, pathogen acquisition occurs during an initial blood meal, leading to colonization of the tick gut, followed by dissemination to the salivary glands. During the next blood meal, pathogens may be transmitted to the vertebrate host via saliva (Kazimírová et al., 2017). The salivary glands can serve as the exit points for pathogen transmission in vector ticks, but in some non-vector ticks, they may also act as barriers to transmission (Ramakrishnan et al., 2005; Yuan et al., 2025b). In *Dermacentor andersoni*, for example, *Anaplasma marginale* subsp. *centrale* colonizes the salivary glands but is not transmitted to the host (Ueti et al., 2007). Bacterial communities within tick salivary glands have been characterized in several species. For example, in *Ixodes scapularis*, *Rickettsia* is the predominant genus, with *Anaplasma*, *Borrelia*, and *Wolbachia* also present (Zolnik

Received: 29 September 2024; Accepted: 30 December 2024; Online: 31 December 2024

Foundation items: This work was supported by the National Natural Science Foundation of China (82102433, 32160124, 32370522, 32090014) and Hainan Provincial Natural Science Foundation of China (822RC711, 821QN254)

[#]Authors contributed equally to this work

*Corresponding authors, E-mail: yuanchuanfei@muhn.edu.cn; zouzhen@ioz.ac.cn; xiaqianfeng@muhn.edu.cn

et al., 2016), while *Staphylococcus* is the predominant salivary gland-associated genus in female *Haemaphysalis longicornis* specimens, followed by *Acinetobacter* and *Ralstonia* (Li et al., 2021b). To the best of our knowledge, however, no studies have explored how the tick salivary gland microbiota responds to pathogen infection.

SFTSV is an emerging tick-borne bunyavirus responsible for SFTS, a disease with a high fatality rate of 12% to 50% in humans. The global incidence of SFTS is rising, raising significant public health concerns, particularly in Asia (Cui et al., 2024; Li et al., 2021a; Yu et al., 2011). Currently, no vaccines or effective therapeutic interventions are available. SFTSV is transmitted via tick bites, with the virus being introduced into hosts through infected tick saliva (Zhuang et al., 2018). *Haemaphysalis longicornis* has been identified as the primary vector for SFTSV (Luo et al., 2015; Zhuang et al., 2018), with *Haemaphysalis flava* (Fang et al., 2023) and *Ixodes sinensis* (Hu et al., 2020) potentially serving as secondary vectors.

Previous studies have established that SFTSV can infect ticks via direct injection and that infected ticks transmit the virus to vertebrates during blood-feeding (Fang et al., 2023; Hu et al., 2020; Yuan et al., 2023; Zhuang et al., 2018). Additionally, our recent study demonstrated that SFTSV infection alters the composition of the gut microbiota in *H. longicornis* (Sun et al., 2024). In this study, SFTSV infection was experimentally established in *H. longicornis* through injection, followed by tick-to-host transmission via feeding on healthy rabbits. Resulting changes in the salivary gland microbiota of *H. longicornis* were investigated using 16S rRNA gene sequencing. Characterizing these shifts in salivary gland bacterial composition associated with SFTSV transmission may facilitate the identification of potential molecular targets for disrupting tick-borne viral transmission and inform epidemiological surveillance strategies for SFTSV.

MATERIALS AND METHODS

Ethics statement

All procedures involving animals were conducted in compliance with the China Laboratory Animal Nursing and Use Regulations and received approval from the Ethics Committee of Hainan Medical University (approval No.: HYLL-2021-393). All viral experiments were performed in a biosafety level 2 laboratory.

Ticks, viruses, and animals

A laboratory colony of *H. longicornis* was maintained under controlled conditions as previously described (Yuan et al., 2020, 2022). Briefly, ticks were fed on a New Zealand white rabbit, and off-host life stages were maintained at 25±1°C with 80%±5% relative humidity. SFTSV Wuhan strain, originally isolated from patient serum, was amplified in Vero cells (Fu et al., 2023). Vero cells were incubated with viral inoculum for 2 h at 37°C, after which the medium was replaced by Dulbecco's modified Eagle's medium (DMEM) (Life Technologies, USA) containing 2% serum. Supernatants were harvested 5 days post-infection, filtered through a 0.45 μm filter, and stored at −80°C. Specific-pathogen-free New Zealand white rabbits (Changsha Tianqin Biotechnology Co., Ltd., Changsha, China) were used for tick feeding and viral transmission experiments.

SFTSV infection and transmission

For SFTSV infection, unfed females were injected intrahemocoelically with 7.25×10^3 focus forming units (FFU) of SFTSV or an equivalent volume (0.5 μL) of phosphate buffered saline (PBS), as described previously (Dong et al., 2019; Yuan et al., 2023, 2025a). Injections were performed between the coxa and trochanter of the fourth leg using the Nanoliter 2020 Injection System (World Precision Instrument, USA). After 14 days, 25 infected female ticks and 15 untreated male ticks were placed on a specific-pathogen-free New Zealand white rabbit for blood-feeding and virus transmission. A control group of 25 uninfected female ticks and 15 untreated male ticks were fed on another rabbit. In total, six rabbits were used in this study.

Sample collection

Four days after tick infestation, 16 female ticks per rabbit were collected and dissected, with their salivary glands isolated following previously established protocols (Patton et al., 2012). Briefly, ticks were rinsed with sterile water, sterilized with 70% ethanol, and dried using sterile paper towels. The ventral side of each tick was affixed to a sterile petri dish using adhesive. The fixed tick was washed several times with sterile PBS, before the dorsal scutum was carefully excised in a circular motion using a sterile stab knife. The salivary glands, recognizable by their grape-like structure, were removed and transferred to a fresh pool of sterile PBS under a dissecting microscope. To minimize contamination, the glands were subsequently washed in three additional sterile PBS pools to remove external microorganisms and debris. Six pairs of salivary glands were pooled for DNA extraction, while 10 pairs were pooled for RNA extraction. Each experimental group consisted of three biological replicates. For serological analysis, rabbit samples were collected at 0, 7, 14, and 21 days post-infestation (dpi) for enzyme-linked immunosorbent assay (ELISA). Each time point included three biological replicates.

qPCR detection of SFTSV in tick salivary glands

Total RNA was extracted using Trizol® Reagent (Invitrogen, USA) and reverse-transcribed into cDNA using HiScript III RT SuperMix for qPCR (Vazyme Biotech, China). The resulting cDNA was subjected to qPCR analysis to assess SFTSV RNA levels. Viral RNA was detected using SFTSV glycoprotein N (Gn) gene-specific primers (Supplementary Table S1). Translation elongation factor 1-alpha (*EF-1α*) from *H. longicornis* served as the internal control gene. Relative viral RNA levels were quantified using the ΔΔ CT method and normalized to *EF-1α* expression.

ELISA

SFTSV-specific antibodies were detected via ELISA. The SFTSV nucleoprotein (NP) gene was amplified from adult tick cDNA and cloned into the pET-28a (+) expression vector for recombinant protein production. Purified recombinant NP (2 μg/mL) in PBS buffer was used to coat ELISA plates, which were incubated overnight at 4°C. After blocking, diluted serum samples (starting at 1:200) were added and incubated at 37°C for 1 h. The plates were then washed three times before incubation with horseradish peroxidase (HRP)-conjugated goat anti-rabbit IgG (1:20 000) (Beyotime, China) at 37°C for 1 h. Following termination of the colorimetric reaction, optical density was measured at 450 nm using a spectrometer (BioTek, USA).

High-throughput sequencing of salivary gland bacterial DNA

Bacterial DNA from tick salivary glands was extracted using a DNeasy Blood & Tissue Kit (Qiagen, USA), following the manufacturer's instructions. Briefly, salivary gland samples were homogenized in buffer ATL, followed by the addition of proteinase K and incubation at 56°C for 1 h to facilitate protein digestion. After digestion, buffer AL and ethanol were sequentially added and mixed. The mixture was then transferred to a DNeasy Mini spin column, and the flow-through was discarded following centrifugation at 8 000 r/min for 1 min at room temperature. To remove proteins and salt ions, the column was sequentially washed with buffer AW1 and buffer AW2. DNA was subsequently eluted twice using buffer AE to ensure optimal recovery.

The V3–V4 hypervariable regions of the 16S rRNA gene were amplified by PCR using the 341F/806R primer pair (Supplementary Table S1) (Hu et al., 2024; Yuan et al., 2021). Sequencing of the products was performed on the Illumina HiSeq platform (BGI-Shenzhen, China).

Sequencing data processing

Paired-end reads (>50 000 reads per sample) generated using the Illumina HiSeq platform were filtrated using cutadapt (v.2.6), readfq (v.1.0), and iTools Fqtools fqcheck (v.0.25) to remove low-quality sequences and adapters. Clean paired-end reads were merged using FLASH (v.1.2.11) with a minimum overlap of 15 bp, yielding high-quality tags. The connectRatio_percent for successfully merged paired-end reads across all samples exceeded 97%. Operational taxonomic units (OTUs) were clustered at 97% sequence identity using USEARCH (v.7.0.1090), with the most abundant sequence in each cluster designated as the representative OTU. Chimeric sequences were identified and removed using UCHIME (v.4.2.40). Taxonomic annotation of representative OTUs was performed against the SILVA database with a confidence level of 60% using RDP classifier (v.2.3). Sample diversity and sequencing depth were assessed using rarefaction curves and Good's coverage estimates.

Bioinformatic analyses

Microbial community diversity was assessed using Mothur (v.1.31.2) and QIIME (v.1.80) to calculate alpha and beta diversities (Caporaso et al., 2010; Schloss et al., 2009). Principal coordinate analysis (PCoA), partial least-squares discriminant analysis (PLS-DA), and heatmap visualization were performed using R (v.4.3.1). Differences in bacterial taxa abundance between control and infected groups were evaluated using the Wilcoxon test, with $P<0.05$ considered statistically significant. Phylogenetic trees were constructed using the neighbor-joining method in MEGA6 (Yuan et al., 2017).

Co-occurrence network analysis

Co-occurrence networks were constructed to assess microbial interactions among genera detected in four or more samples using the R "ggClusterNet" package and Gephi software (v.0.10.1). Correlations were calculated using the ggClusterNet package in R (Wen et al., 2022), applying a stringent threshold of $|r|>0.6$ and $P<0.01$ to ensure statistical robustness and network stability. Co-occurrence network patterns were analyzed using Gephi, with node size representing the number of interactions (edges) per genus.

Statistical analysis

Statistical analyses for qPCR and ELISA data were conducted using GraphPad v.8 software. Differences between two groups were analyzed using two-tailed Student's *t*-tests, with significance defined at *: $P<0.05$ and **: $P<0.01$.

RESULTS

Tick-to-host transmission of SFTSV

To determine whether *H. longicornis* transmits SFTSV to rabbit hosts through blood-feeding, infected female ticks were allowed to feed on specific pathogen-free rabbits. During the adult transmission phase, salivary glands from partially fed females were collected for viral RNA detection, and serum samples were obtained from the rabbits (Figure 1A). Analysis revealed that the relative SFTSV RNA levels in the salivary glands of infected females exceeded 6-fold, normalized to *EF-1α* expression (Figure 1B). In contrast, no SFTSV RNA was detected in the salivary glands of ticks from the control group. Serological analysis using ELISA demonstrated a significant increase (>12-fold) in SFTSV NP-specific antibody levels in rabbits exposed to infected tick bites at 21 dpi (Figure 1C). Antibody levels in the control group did not differ significantly between time points. Collectively, these results confirm that SFTSV can be efficiently transmitted to rabbits via tick feeding.

Bacterial 16S rRNA profiles in *H. longicornis* salivary glands

To characterize the bacterial communities in tick salivary glands, partially fed female *H. longicornis* were collected for 16S rRNA sequencing. Sequencing generated between 52 629 to 78 261 paired-end reads from mock-infected and SFTSV-infected samples (Supplementary Table S2), resulting in 50 879–73 834 high-quality clean tags after filtration. Taxonomic annotations identified a total of 251 OTUs, 70 of which were shared between control and infected groups, while 55 were specific to the infected group (Figure 2A).

Rarefaction curve analysis demonstrated that sequencing depth reached a saturation plateau between 1 000 and 20 000 sequences per sample (Figure 2B). Additionally, Good's coverage estimator values for each sample approached 100% (>99.9%), confirming adequate sequencing depth for comprehensive microbiota profiling.

Bacterial composition of *H. longicornis* salivary glands

A comprehensive taxonomic analysis of the salivary gland microbiota identified 14 phyla, 24 classes, 41 orders, 79 families, and 124 genera across six samples. At the phylum level, Proteobacteria dominated the bacterial community in both groups, increasing from 91.80% in the control group to 96.97% in the infected group (Figure 3A). Other phyla with relative abundances exceeding 0.5% in the control group included Actinobacteria (3.29%), Firmicutes (2.40%), and Bacteroidetes (0.99%), which decreased to 1.62%, 1.23%, and 0.07% in the infected group. Notably, Parcubacteria was identified exclusively in the control group.

At the genus level, *Coxiella* was the predominant taxon, accounting for 81.32% of identified sequences in the control group, increasing to 92.06% in the infected group (Figure 3B). Other genera with relative abundances exceeding 0.5% in the control group included *Brevibacterium* (1.98%), *Stenotrophomonas* (2.04%), and *Massilia* (1.45%), which decreased to 0.35%, 0.008%, and undetectable in the infected

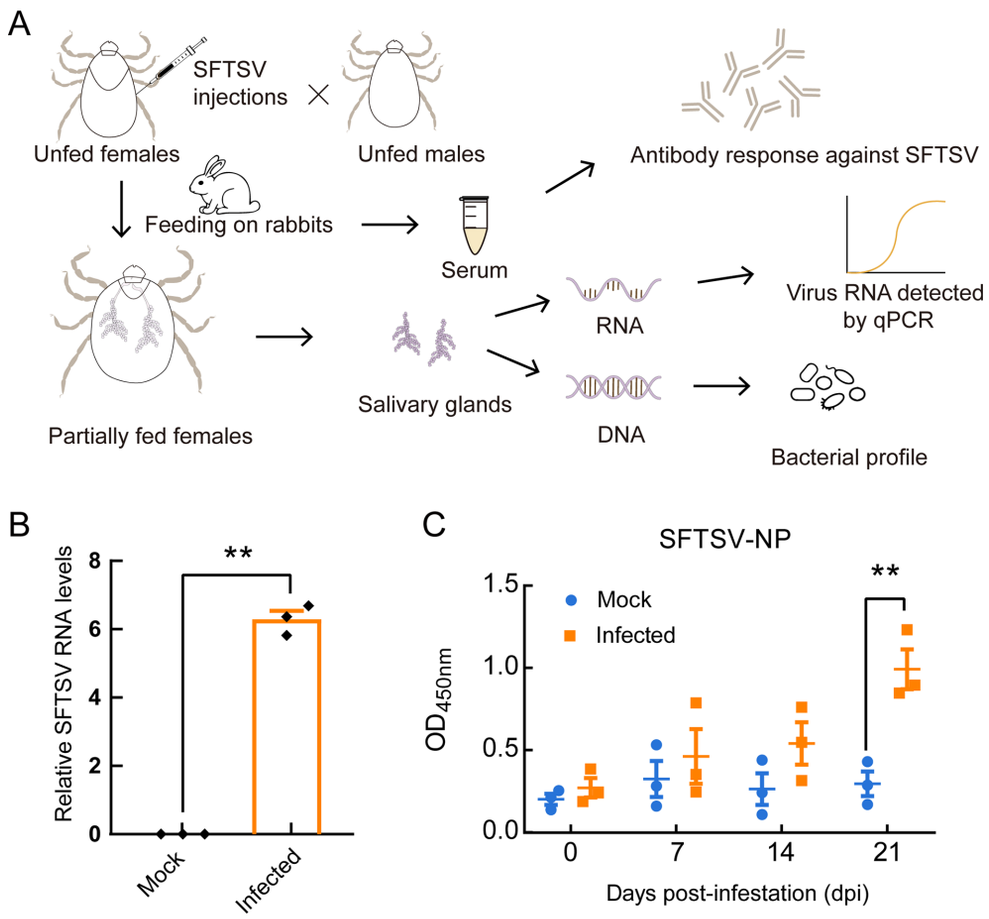

Figure 1 Tick-to-host transmission of severe fever with thrombocytopenia syndrome virus (SFTSV) in naïve rabbits

A: Schematic overview of study design. B: Detection of SFTSV RNA in salivary glands of partially fed ticks. Mock, salivary glands from mock-infected female ticks. Infected, salivary glands from infected female ticks. C: Induction of anti-nucleoprotein (NP) antibodies in rabbits following tick infestation. Mock, serum samples from rabbits exposed to mock-infected female ticks. Infected, serum samples from rabbits exposed to infected female ticks. Data are presented as mean±standard error of the mean (SEM) of three biological repeats. Statistical significance was determined using two-tailed Student's *t*-tests. *: $P<0.05$; **: $P<0.01$.

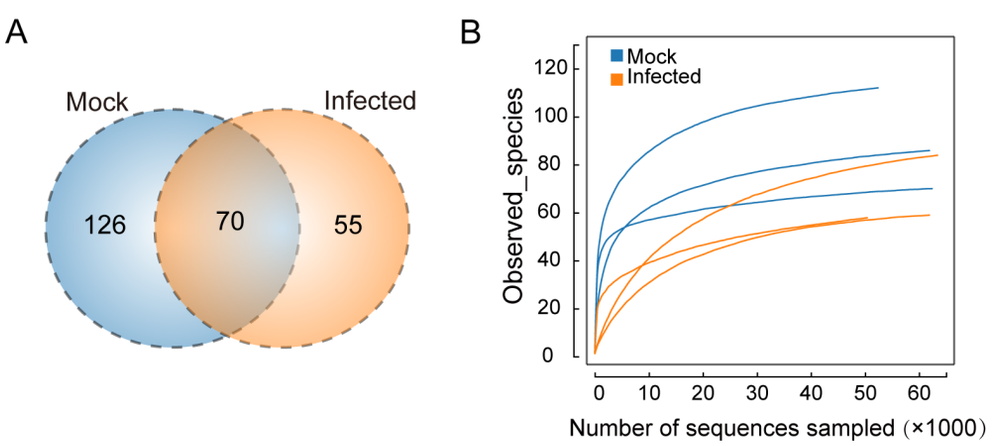

Figure 2 Venn diagram and rarefaction analysis of *Haemaphysalis longicornis* salivary gland samples

A: Venn diagram of observed OTUs in salivary gland samples. Mock, salivary gland samples prepared from partially fed females without SFTSV infection. Infected, salivary gland samples prepared from partially fed females infected with SFTSV. B: Rarefaction analysis of salivary gland samples.

group. Interestingly, *Serratia*, absent in the control group, emerged in the infected group, constituting 1.03% of the total bacterial community. Additionally, *Micrococcus* and *Pseudomonas*, which were present at 0.25% and 0.36% in the control group, increased to 1.03% and 0.51%, respectively, upon infection.

Bacterial diversity in *H. longicornis* salivary glands

Alpha diversity was assessed using Chao, abundance-based coverage estimator (ACE), Shannon, and Simpson indices. Three of these indices decreased in the infected group (78.66,

78.16, and 0.42, respectively) compared with the control group (94.77, 97.21, and 1.09, respectively) (Table 1), while the Simpson index increased from 0.66 in the control group to 0.86 in the infected group. However, Wilcoxon test results indicated that these changes were not statistically significant, suggesting that SFTSV infection did not significantly alter the overall alpha diversity of the salivary gland bacteriome.

Beta diversity was evaluated using PCoA and PLS-DA at the OTU level. PCoA based on weighted UniFrac distances identified two principal components (PCoA1 and PCoA2), which together explained 82.43% of the variation (Figure 4A). The bacterial communities from the control and infected groups formed distinct clusters in the PCoA plot. Similarly, PLS-DA demonstrated clear separation between the bacterial communities of infected and control groups, suggesting a significant shift in bacterial composition following SFTSV infection. Although minor variations were observed among biological replicates within the infected group, the overall bacterial community structure differed markedly from the control group (Figure 4B).

Viral infection alters bacterial communities in *H. longicornis*

To identify differences in bacterial taxa between the control and infected groups, a linear discriminant analysis (LDA) effect size (LEfSe) algorithm was applied. A total of eight bacterial genera exhibited significant differences in abundance between groups. Among these, *Serratia*, *Bifidobacterium*, and *Akkermansia* were enriched in the infected group, while *Flavobacterium*, *Staphylococcus*, *Enhydrobacter*, *Massilia*, and *Stenotrophomonas* were depleted (Figure 5A). *Serratia* and *Bifidobacterium* were detected exclusively in the infected group, while *Massilia* was present only in the control group (Figure 5B). Taxonomic resolution at the OTU level revealed that OTU19, classified as *Serratia marcescens*, was the only OTU identified for the *Serratia* genus, while OTU174, assigned to *Akkermansia muciniphila*, was the sole representative of *Akkermansia* (Figure 5C).

Microbiota network interactions in response to SFTSV infection

To explore bacterial interactions within the salivary gland bacteriome, correlation networks were established based on genus-level abundance. In the control group, the co-occurrence network comprised 41 nodes and 197 edges, with *Staphylococcus*, *Enhydrobacter*, *Massilia*, and *Stenotrophomonas* clustering within the same subcommunity (Figure 6A). Notably, *Akkermansia* exhibited a negative correlation with *Flavobacterium* in a separate subcommunity. In the infected group, the co-occurrence network included 43 nodes and 217 edges, with *Akkermansia* also exhibiting a negative correlation with *Flavobacterium* (Figure 6B). In addition, *Serratia*, *Bifidobacterium*, *Enhydrobacter*, and *Stenotrophomonas* formed an interconnected subcommunity. These findings suggest that SFTSV infection alters microbial interactions, increasing the complexity of the salivary gland microbiota network.

DISCUSSION

This study represents the first investigation into SFTSV-induced alterations in the tick salivary gland microbiota. Our findings suggest that these microbial shifts may influence tick-to-host transmission of SFTSV. Previous studies have primarily focused on changes in the gut microbiota following host-to-tick transmission of tick-borne pathogens (Adegoke et al., 2022; Mahmood et al., 2021; Omondi et al., 2023). Here, we demonstrated that SFTSV transmission from tick to host significantly altered salivary gland microbial composition, with three genera (*Serratia*, *Bifidobacterium*, and *Akkermansia*) enriched and five genera *(Flavobacterium*,

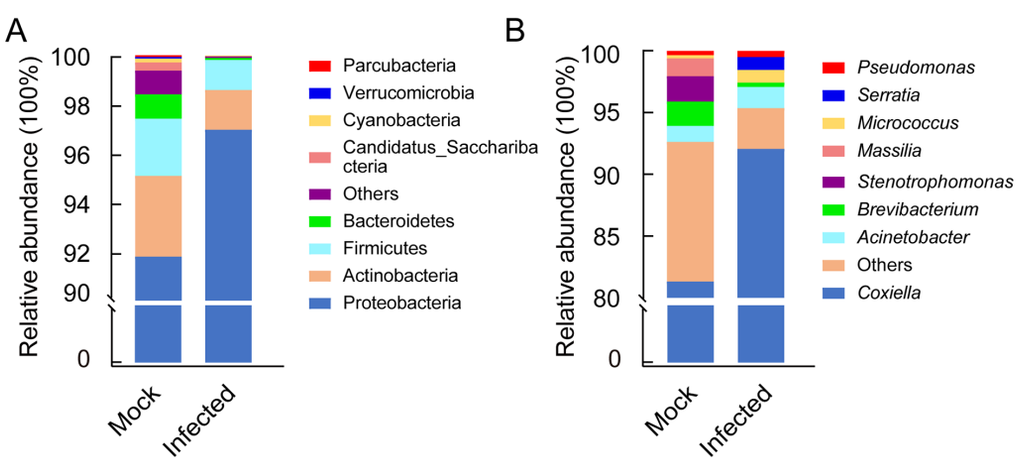

Figure 3 Taxonomic diversity and abundance of six sequenced samples at the phylum (A) and genus (B) levels

Table 1 Alpha diversity metrics for individual samples from the control and infected groups

Sample	Chao	ACE	Shannon	Simpson
Mock1	91.5	95.520087	0.841982	0.713695
Mock2	119.8	120.722966	1.26119	0.623253
Mock3	73	75.383971	1.167226	0.656401
Infected1	84.25	75.341085	1.047461	0.634589
Infected2	62.272727	64.175401	0.133693	0.958337
Infected3	89.454545	94.974604	0.093788	0.978761

ACE: Abundance-based coverage estimator.

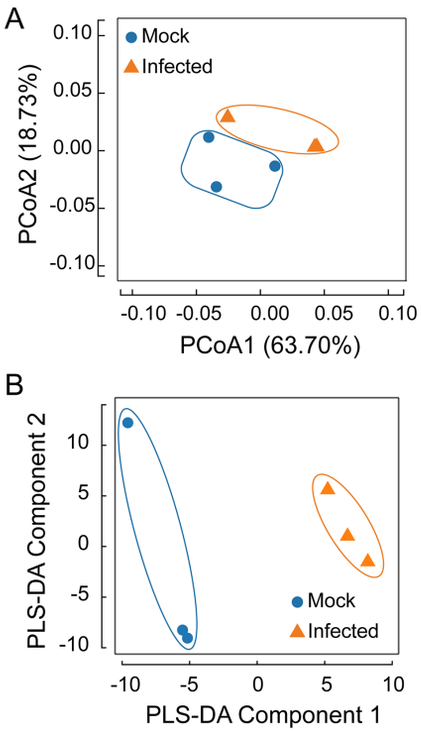

Figure 4 Principal coordinates analysis (PCoA) and partial least-squares discrimination analysis (PLS-DA) of bacterial communities in salivary gland samples

A: PCoA plots based on weighted UniFrac metrics for bacterial communities in mock and infected samples. B: PLS-DA results for bacterial communities in mock and infected samples.

Staphylococcus, *Enhydrobacter*, *Massilia*, and *Stenotrophomonas*) depleted in infected ticks. With the advancement of anti-microbiota vaccines enabling taxon-specific manipulation of tick-associated bacteria (Mateos-Hernández et al., 2020, 2021), further investigation into the roles of these taxa in SFTSV transmission may provide novel strategies for SFTS control.

Pathogen infection is known to modulate arthropod microbiota composition (Xiong et al., 2024). We previously found that baculovirus infection increases *Enterococcus* abundance in the midgut of *Helicoverpa armigera* (Yuan et al., 2021). Furthermore, introduction of *Enterococcus* into the gut of germ-free *H. armigera* has been shown to enhance larval survival following baculovirus infection, likely due to the restoration of baseline immune function (Tian et al., 2023). Similarly, in *I. scapularis*, *Anaplasma phagocytophilum* infection has been shown to increase *Pseudomonas* abundance and reduce *Enterococcus* and *Rickettsia* levels in nymphs (Abraham et al., 2017), while *Borrelia burgdorferi* infection correlates with elevated *Bacillus* and *Pseudomonas* levels in the tick gut (Ross et al., 2018). Gut microbiota disruption in ticks can compromise the peritrophic matrix and gut barrier, which serve as essential defenses against *Anaplasma* colonization (Abraham et al., 2017). In *Dermacentor occidentalis* ticks, *Rickettsia bellii* levels are negatively correlated with *A. marginale* levels (Gall et al., 2016). Two possible mechanisms have been proposed for rickettsial interference: (i) inhibition of *A. marginale* replication by a molecule released by *R. bellii*, and (ii) competition for host-derived resources essential for *A. marginale* replication (Gall et al., 2016). Our findings further support the notion that pathogen infection modulates arthropod microbiota composition. These microbial alterations may influence SFTSV transmission through multiple mechanisms, including modulation of tick immunity, disruption of the salivary gland barrier, or competition for host resources required for viral replication.

Coxiella, a maternally inherited endosymbiont, is essential for tick development and reproduction, with its reduced abundance impairing blood-feeding efficiency and reproductive fitness in *H. longicornis* (Zhang et al., 2017; Zhong et al., 2021). In addition to its role in tick physiology, *Coxiella* may facilitate transstadial transmission of *Babesia microti* from larvae to nymphs in *Rhipicephalus haemaphysaloides* (Li et al., 2018). Previous studies have also identified coinfection of *Coxiella* and SFTSV in *H. longicornis* (Yoo et al., 2023). Our findings confirmed *Coxiella* as the predominant bacterial taxon in the salivary glands of *H. longicornis*, with SFTSV infection shown to increase its relative abundance, albeit non-significantly, consistent with previous observations in *H. longicornis* (Sun et al., 2024). These results suggest that *Coxiella* may influence SFTSV infection and transmission, potentially by modulating tick fitness.

In this study, only a single *Serratia* OTU was detected, corresponding to *S. marcescens*. In *Aedes aegypti*, *S. marcescens* facilitates arboviral dissemination by digesting gut membrane-bound mucins through its secreted protein SmEnhancin (Wu et al., 2019). Conversely, in *Anopheles stephensi*, *S. marcescens* suppresses *Plasmodium berghei* infection by activating mosquito immune responses (Bai et al., 2019). Moreover, in houseflies, *S. marcescens* modulates host development by interfering with gut microbiota composition (Li et al., 2023). This bacterium has also been documented in *Amblyomma cajennense*, *Rhipicephalus microplus*, and *D. andersoni* tick eggs (Andreotti et al., 2011; Machado-Ferreira et al., 2015; Steinhaus, 1942) and has been isolated from intestinal tissues and hemolymph of *R. microplus* (Molina-Garza and Galaviz-Silva, 2020). Notably, in this study, *S. marcescens* was exclusively detected in the salivary glands of SFTSV-infected ticks, implying that it may contribute to tick-to-host transmission of SFTSV. Given that *S. marcescens* promotes viral dissemination in mosquitoes via SmEnhancin-mediated degradation of epithelial barriers, future investigations should explore whether SmEnhancin facilitates SFTSV transmission by compromising the tick salivary gland barrier, thereby enhancing viral release into the vertebrate host.

Only a single *Akkermansia* OTU corresponding to *A. muciniphila* was identified in this study. This bacterium is a well-characterized gut bacterium known for its ability to degrade mucin (Geerlings et al., 2018) and is inversely associated with inflammatory responses (Earley et al., 2019). In the context of mosquito-borne viral transmission, host inflammatory responses to mosquito bites can enhance viral infection (Pingen et al., 2016). Similarly, in tick-borne viruses, virus-infected ticks induce localized inflammation at the murine cutaneous interface, which may facilitate viral entry by recruiting host immune cells to the bite site (Hermance et al., 2016; Hermance and Thangamani, 2014; Thangamani et al., 2017). More recently, *A. muciniphila* has been reported to protect mice against SFTSV by producing the β-carboline alkaloid harmaline, which suppresses systemic inflammation (Xie et al., 2023). The increased abundance of *A. muciniphila*

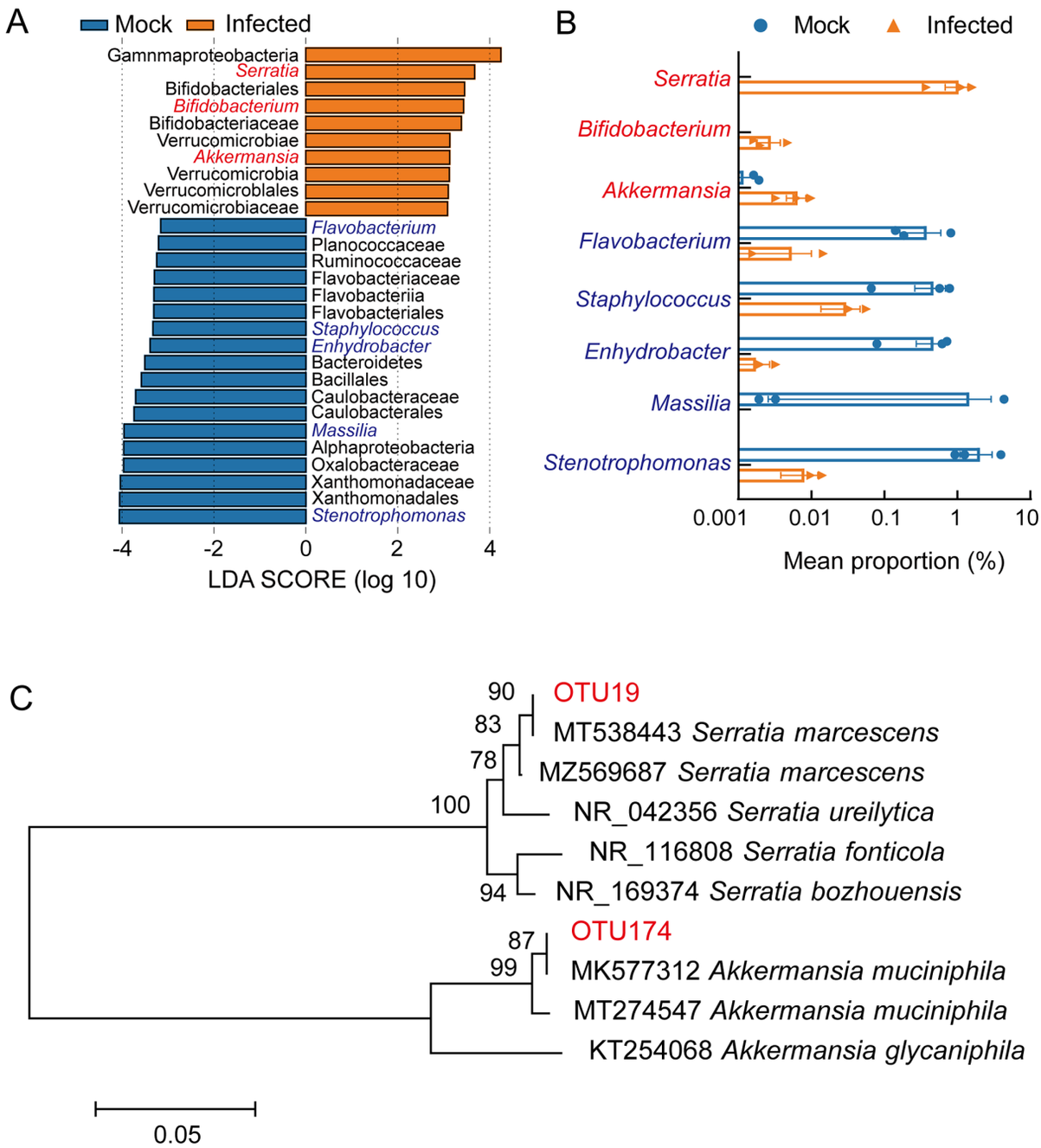

Figure 5 Identification of differentially abundant taxa in tick salivary glands using linear discriminant analysis (LDA) effect size (LEfSe) analysis

A: Histogram of LDA scores showing genera with significantly different abundances between control and infected salivary gland samples. Blue, enriched in mock group. Yellow, enriched in infected group. B: Relative abundance of bacterial genera enriched in salivary glands of control and infected female ticks. C: Phylogenetic tree constructed from 16S rRNA gene sequences, showing the phylogenetic relationships of the identified *Akkermansia muciniphila* and *Serratia marcescens* OTUs.

in SFTSV-infected tick salivary glands and its negative correlation with *Flavobacterium* suggest that this bacterium may play a previously unrecognized role in SFTSV transmission, warranting further investigation.

We previously identified *Massilia*, a genus of Gram-negative bacteria, as a predominant bacterial taxon in field-collected *Haemaphysalis* ticks (Lu et al., 2023). Certain *Massilia* species can produce antimicrobial compounds (Dahal et al., 2021). *Bifidobacterium*, a genus of Gram-positive bacteria, includes species known to cause opportunistic infections in humans (Butta et al., 2017). In *Dermacentor silvarum*, *Bifidobacterium* has been detected exclusively in saliva, suggesting that it may be directly transmitted to mammalian hosts during blood-feeding (Duan et al., 2020). Other bacterial genera identified in this study may also have implications for SFTSV transmission. *Stenotrophomonas*, a Gram-negative genus, includes opportunistic pathogens capable of causing infections in humans (Kanderi et al., 2020). *Enhydrobacter* and *Staphylococcus* are components of the healthy human skin microbiota (Kim et al., 2021). The significant shifts in the relative abundance of these bacteria in tick salivary glands following SFTSV infection suggest potential interactions with

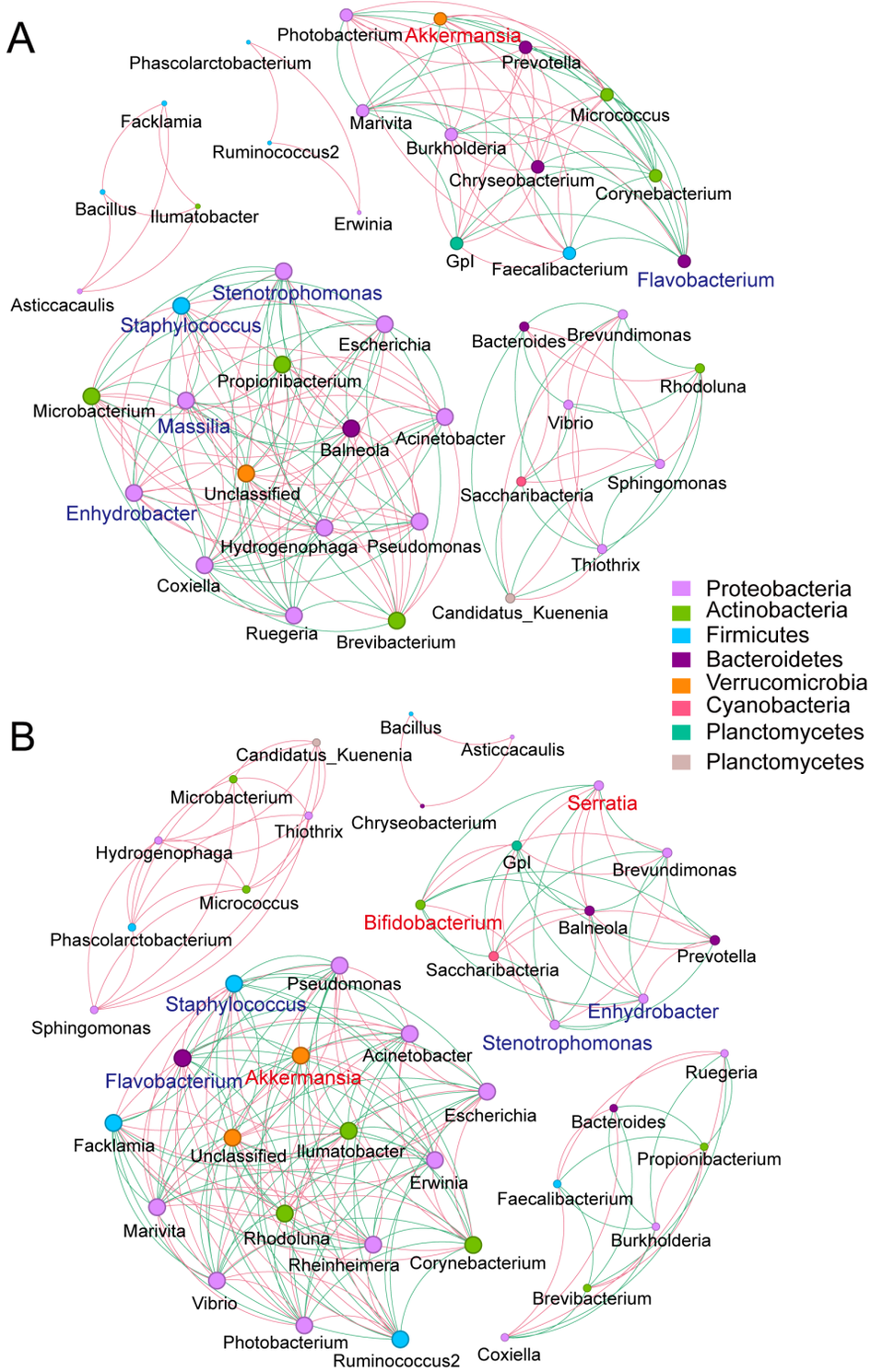

Figure 6 Genus-level bacterial co-occurrence networks based on correlation analysis

A, B: Bacterial interaction networks for mock (A) and infected (B) groups constructed using Gephi. Nodes indicate OTUs labeled with their corresponding bacterial genera. Red edges indicate positive correlations, while green edges indicate negative correlations. Genera enriched in the infected and mock groups are highlighted in red and blue, respectively.

viral transmission dynamics. Whether their depletion impairs functions that inhibit viral transmission remains an open question for future research.

A key limitation of this study is the small sample size, which may constrain the generalizability of the findings. In addition, whether SFTSV-induced alterations in the salivary gland microbiota of *H. longicornis* are conserved across different mammalian hosts remains unknown. The potential role of these microbial shifts in facilitating viral transmission also warrants further investigation. Despite these limitations, this study provides the first comprehensive analysis of bacterial dynamics in the salivary glands of *H. longicornis* during tick-to-host SFTSV transmission. These findings lay the groundwork for future microbiota-focused studies on SFTSV transmission

and may enhance our understanding of tick-virus-host interactions, revealing potential biomarkers of SFTSV infection and transmission in endemic areas.

DATA AVAILABILITY

The 16S rRNA deep sequencing data generated in this study were deposited in the Genome Sequence Archive (GSA) database (PRJCA034557), Science Data Bank (DOI: 10.57760/sciencedb.j00139.00156), and Sequence Read Archive of the National Center for Biotechnology Information (BioProjectID PRJNA1047962).

SUPPLEMENTARY DATA

Supplementary data to this article can be found online.

COMPETING INTERESTS

The authors declare that they have no competing interests.

AUTHORS' CONTRIBUTIONS

Q.X., Z.Z., and C.Y. designed the experiments; J.C., C.Y., Q.X., Y.S., R.Z., C.Z., Y.W., Z.Z., and Q.X. assisted with the experiments and provided intellectual input; Q.X., Z.Z., and C.Y. supervised the study; J.C., C.Y., Q.X., Z.Z., and Q.X. interpreted the data and wrote the manuscript. All authors read and approved the final version of the manuscript.

REFERENCES

Abraham NM, Liu L, Jutras BL, et al. 2017. Pathogen-mediated manipulation of arthropod microbiota to promote infection. *Proceedings of the National Academy of Sciences of the United States of America*, **114**(5): E781–E790.

Adegoke A, Kumar D, Budachetri K, et al. 2022. Hematophagy and tick-borne rickettsial pathogen shape the microbial community structure and predicted functions within the tick vector, *Amblyomma maculatum*. *Frontiers in Cellular and Infection Microbiology*, **12**: 1037387.

Andreotti R, Pérez de León AA, Dowd SE, et al. 2011. Assessment of bacterial diversity in the cattle tick *Rhipicephalus (Boophilus) microplus* through tag-encoded pyrosequencing. *BMC Microbiology*, **11**(1): 6.

Bai L, Wang LL, Vega-Rodriguez J, et al. 2019. A gut symbiotic bacterium *Serratia marcescens* renders mosquito resistance to *Plasmodium* infection through activation of mosquito immune responses. *Frontiers in Microbiology*, **10**: 1580.

Butta H, Sardana R, Vaishya R, et al. 2017. Bifidobacterium: an emerging clinically significant metronidazole-resistant anaerobe of mixed pyogenic infections. *Cureus*, **9**(4): e1134.

Caporaso JG, Kuczynski J, Stombaugh J, et al. 2010. QIIME allows analysis of high-throughput community sequencing data. *Nature Methods*, **7**(5): 335–336.

Cui HL, Shen SJ, Chen L, et al. 2024. Global epidemiology of severe fever with thrombocytopenia syndrome virus in human and animals: a systematic review and meta-analysis. *The Lancet Regional Health-Western Pacific*, **48**: 101133.

Dahal RH, Chaudhary DK, Kim J. 2021. Genome insight and description of antibiotic producing *Massilia antibiotica* sp. nov. , isolated from oil-contaminated soil. *Scientific Reports*, **11**(1): 6695.

Dong FF, Li DD, Wen D, et al. 2019. Single dose of a rVSV-based vaccine elicits complete protection against severe fever with thrombocytopenia syndrome virus. *npj Vaccines*, **4**: 5.

Duan DY, Liu GH, Cheng TY. 2020. Microbiome analysis of the saliva and midgut from partially or fully engorged female adult *Dermacentor silvarum* ticks in China. *Experimental and Applied Acarology*, **80**(4): 543–558.

Earley H, Lennon G, Balfe Á, et al. 2019. The abundance of *Akkermansia muciniphila* and its relationship with sulphated colonic mucins in health and ulcerative colitis. *Scientific Reports*, **9**(1): 15683.

Fang LZ, Xiao X, Lei SC, et al. 2023. *Haemaphysalis flava* ticks as a competent vector of severe fever with thrombocytopenia syndrome virus. *Ticks and Tick-Borne Diseases*, **14**(2): 102100.

Fu HM, Wang YH, Yuan CF, et al. 2023. Screening core genes and signaling pathways after SFTSV infection by integrated transcriptome profiling analysis. *Virus Research*, **332**: 199138.

Gall CA, Reif KE, Scoles GA, et al. 2016. The bacterial microbiome of *Dermacentor andersoni* ticks influences pathogen susceptibility. *The ISME Journal*, **10**(8): 1846–1855.

Geerlings SY, Kostopoulos I, De Vos WM, et al. 2018. *Akkermansia muciniphila* in the human gastrointestinal tract: when, where, and how?. *Microorganisms*, **6**(3): 75.

Hermance ME, Santos RI, Kelly BC, et al. 2016. Immune cell targets of infection at the tick-skin interface during Powassan virus transmission. *PLoS One*, **11**(5): e0155889.

Hermance ME, Thangamani S. 2014. Proinflammatory cytokines and chemokines at the skin interface during Powassan virus transmission. *Journal of Investigative Dermatology*, **134**(8): 2280–2283.

Hu B, Wang JM, Zhang QX, et al. 2024. *Enterococcus faecalis* provides protection during scavenging in carrion crow (*Corvus corone*). *Zoological Research*, **45**(3): 451–463.

Hu YY, Zhuang L, Liu K, et al. 2020. Role of three tick species in the maintenance and transmission of severe fever with thrombocytopenia syndrome virus. *PLoS Neglected Tropical Diseases*, **14**(6): e0008368.

Jia N, Wang JF, Shi WQ, et al. 2020. Large-scale comparative analyses of tick genomes elucidate their genetic diversity and vector capacities. *Cell*, **182**(5): 1328–1340. e13.

Kanderi T, Shrimanker I, Mansoora Q, et al. 2020. *Stenotrophomonas maltophilia*: an emerging pathogen of the respiratory tract. *American Journal of Case Reports*, **21**: e921466.

Kazimírová M, Thangamani S, Bartíková P, et al. 2017. Tick-borne viruses and biological processes at the tick-host-virus interface. *Frontiers in Cellular and Infection Microbiology*, **7**: 339.

Kim JH, Son SM, Park H, et al. 2021. Taxonomic profiling of skin microbiome and correlation with clinical skin parameters in healthy Koreans. *Scientific Reports*, **11**(1): 16269.

Li J, Li S, Yang L, et al. 2021a. Severe fever with thrombocytopenia syndrome virus: a highly lethal bunyavirus. *Critical Reviews in Microbiology*, **47**(1): 112–125.

Li LH, Zhang Y, Zhu D, et al. 2018. Endosymbionts alter larva-to-nymph transstadial transmission of *Babesia microti* in *Rhipicephalus haemaphysaloides* ticks. *Frontiers in Microbiology*, **9**: 1415

Li SS, Zhang XY, Zhou XJ, et al. 2021b. Bacterial microbiota analysis demonstrates that ticks can acquire bacteria from habitat and host blood meal. *Experimental and Applied Acarology*, **87**(1): 81–95.

Li Y, Wang SM, Zhang KX, et al. 2023. *Serratia marcescens* in the intestine of housefly larvae inhibits host growth by interfering with gut microbiota. *Parasites & Vectors*, **16**(1): 196.

Lu YJ, Yang SQ, Zhao QY, et al. 2023. Diversity analysis of the endosymbiotic bacterial community in field-collected *Haemaphysalis ticks* on the tropical Hainan Island, China. *Folia Parasitologica*, **70**: 012.

Luo LM, Zhao L, Wen HL, et al. 2015. *Haemaphysalis longicornis* ticks as reservoir and vector of severe fever with thrombocytopenia syndrome virus in China. *Emerging Infectious Diseases*, **21**(10): 1770–1776.

Machado-Ferreira E, Dietrich G, Hojgaard A, et al. 2011. *Coxiella* symbionts in the Cayenne tick *Amblyomma cajennense*. *Microbial Ecology*, **62**(1): 134–142.

Machado-Ferreira E, Vizzoni VF, Piesman J, et al. 2015. Bacteria associated with *Amblyomma cajennense* tick eggs. *Genetics and Molecular Biology*, **38**(4): 477–483.

Mahmood S, Sima R, Urbanova V, et al. 2021. Identification of tick *Ixodes ricinus* midgut genes differentially expressed during the transmission of *Borrelia afzelii* spirochetes using a transcriptomic approach. *Frontiers in Immunology*, **11**: 612412.

Mateos-Hernández L, Obregón D, Maye J, et al. 2020. Anti-tick microbiota vaccine impacts *Ixodes ricinus* performance during feeding. *Vaccines*, **8**(4): 702.

Mateos-Hernández L, Obregón D, Wu-Chuang A, et al. 2021. Anti-microbiota vaccines modulate the tick microbiome in a taxon-specific manner. *Frontiers in Immunology*, **12**: 704621.

Molina-Garza ZJ, Galaviz-Silva L. 2020. Cultivable bacteria isolated from cattle ticks of Nuevo León and Zacatecas, Mexico, and an assessment of their antagonism against bacteria of clinical concern. *International Journal of Acarology*, **46**(1): 41–47.

Narasimhan S, Rajeevan N, Liu L, et al. 2014. Gut microbiota of the tick vector *Ixodes scapularis* modulate colonization of the Lyme disease spirochete. *Cell Host & Microbe*, **15**(1): 58–71.

Omondi D, Zweygarth E, Murungi E, et al. 2023. De novo assembly and annotation of the *Amblyomma hebraeum* tick midgut transcriptome response to *Ehrlichia ruminantium* infection. *PLoS Neglected Tropical Diseases*, **17**(8): e0011554.

Patton TG, Dietrich G, Brandt K, et al. 2012. Saliva, salivary gland, and hemolymph collection from Ixodes scapularis ticks. *Journal of Visualized Experiments*, **21**(60): 3894.

Pingen M, Bryden SR, Pondeville E, et al. 2016. Host inflammatory response to mosquito bites enhances the severity of arbovirus infection. *Immunity*, **44**(6): 1455–1469.

Ramakrishnan VG, Aljamali MN, Sauer JR, et al. 2005. Application of RNA interference in tick salivary gland research. *Journal of Biomolecular Techniques*, **16**(4): 297–305.

Ross BD, Hayes B, Radey MC, et al. 2018. *Ixodes scapularis* does not harbor a stable midgut microbiome. *The ISME Journal*, **12**(11): 2596–2607.

Schloss PD, Westcott SL, Ryabin T, et al. 2009. Introducing mothur: open-source, platform-independent, community-supported software for describing and comparing microbial communities. *Applied and Environmental Microbiology*, **75**(23): 7537–7541.

Steinhaus EA. 1942. The microbial flora of the rocky mountain wood tick, *Dermacentor andersoni* stiles. *Journal of Bacteriology*, **44**(4): 397–404.

Sun Y, Chen C, Zeng CH, et al. 2024. Severe fever with thrombocytopenia syndrome virus infection shapes gut microbiome of the tick vector *Haemaphysalis longicornis*. *Parasites & Vectors*, **17**(1): 107.

Thangamani S, Hermance ME, Santos RI, et al. 2017. Transcriptional immunoprofiling at the tick-virus-host interface during early stages of tick-borne encephalitis virus transmission. *Frontiers in Cellular and Infection Microbiology*, **7**: 494.

Tian ZQ, Guo X, Michaud JP, et al. 2023. The gut microbiome of *Helicoverpa armigera* enhances immune response to baculovirus infection via suppression of duox-mediated reactive oxygen species. *Pest Management Science*, **79**(10): 3611–3621.

Tsementzi D, Castro Gordillo J, Mahagna M, et al. 2018. Comparison of closely related, uncultivated *Coxiella* tick endosymbiont population genomes reveals clues about the mechanisms of symbiosis. *Environmental Microbiology*, **20**(5): 1751–1764.

Ueti MW, Reagan JO Jr, Knowles DP Jr, et al. 2007. Identification of midgut and salivary glands as specific and distinct barriers to efficient tick-borne transmission of *Anaplasma marginale*. *Infection and Immunity*, **75**(6): 2959–2964.

Wen T, Xie PH, Yang SD, et al. 2022. ggClusterNet: an R package for microbiome network analysis and modularity-based multiple network layouts. *iMeta*, **1**(3): e32.

Wu P, Sun P, Nie KX, et al. 2019. A gut commensal bacterium promotes mosquito permissiveness to arboviruses. *Cell Host & Microbe*, **25**(1): 101–112. e5.

Wu-Chuang A, Mateos-Hernandez L, Maitre A, et al. 2023. Microbiota perturbation by anti-microbiota vaccine reduces the colonization of *Borrelia afzelii* in *Ixodes ricinus*. *Microbiome*, **11**(1): 151.

Xie JY, Li H, Zhang XA, et al. 2023. *Akkermansia muciniphila* protects mice against an emerging tick-borne viral pathogen. *Nature Microbiology*, **8**(1): 91–106.

Xiong JB, Sha HN, Chen J. 2024. Updated roles of the gut microbiota in exploring shrimp etiology, polymicrobial pathogens, and disease incidence. *Zoological Research*, **45**(4): 910–923.

Yoo JR, Heo ST, Kim M, et al. 2023. Coinfection of severe fever with thrombocytopenia syndrome virus and *Coxiella burnetii* in developmental stage of hard ticks in subtropical region of Korea. *Journal of Korean Medical Science*, **38**(20): e156.

Yu XJ, Liang MF, Zhang SY, et al. 2011. Fever with thrombocytopenia associated with a novel bunyavirus in China. *New England Journal of Medicine*, **364**(16): 1523–1532.

Yuan CF, Lu YJ, Li JQ, et al. 2023. Infection and transovarial transmission of severe fever with thrombocytopenia syndrome virus in *Rhipicephalus sanguineus* in Hainan Island, China. *Integrative Zoology*, **18**(6): 1009–1013.

Yuan CF, Sun Y, Chen JJ, et al. 2025a. *Haemaphysalis longicornis* subolesin controls the infection and transmission of severe fever with thrombocytopenia syndrome virus. *npj Vaccines*, **10**(1): 17.

Yuan CF, Wu J, Peng Y, et al. 2020. Transcriptome analysis of the innate immune system of *Hyalomma asiaticum*. *Journal of Invertebrate Pathology*, **177**: 107481.

Yuan CF, Xing LS, Wang ML, et al. 2017. Inhibition of melanization by serpin-5 and serpin-9 promotes baculovirus infection in cotton bollworm *Helicoverpa armigera*. *PLoS Pathogens*, **13**(9): e1006645.

Yuan CF, Xing LS, Wang ML, et al. 2021. Microbiota modulates gut immunity and promotes baculovirus infection in *Helicoverpa armigera*. *Insect Science*, **28**(6): 1766–1779.

Yuan CF, Xu Q, Ning YJ, et al. 2025b. Potential mechanisms implied in tick infection by arboviruses and their transmission to vertebrate hosts. *Integrative Zoology*, **20**(2): 315–330.

Yuan CF, Yang QT, Wu J, et al. 2022. Proteomics reveals the hemolymph components of partially fed *Hyalomma asiaticum* ticks. *Ticks and Tick-Borne Diseases*, **13**(6): 102032.

Zhang CM, Li NX, Zhang TT, et al. 2017. Endosymbiont CLS-HI plays a role in reproduction and development of *Haemaphysalis longicornis*. *Experimental and Applied Acarology*, **73**(3-4): 429–438.

Zhang YK, Li SS, Yang C, et al. 2024. Tetracycline inhibits tick host reproduction by modulating bacterial microbiota, gene expression and metabolism levels. *Pest Management Science*, **80**(2): 366–375.

Zhong ZW, Zhong T, Peng YQ, et al. 2021. Symbiont-regulated serotonin biosynthesis modulates tick feeding activity. *Cell Host & Microbe*, **29**(10): 1545–1557. e4.

Zhuang L, Sun Y, Cui XM, et al. 2018. Transmission of severe fever with thrombocytopenia syndrome virus by *Haemaphysalis longicornis* ticks, China. *Emerging Infectious Diseases*, **24**(5): 868–871.

Zolnik CP, Prill RJ, Falco RC, et al. 2016. Microbiome changes through ontogeny of a tick pathogen vector. *Molecular Ecology*, **25**(19): 4963–4977.